

Fractal Properties of Solar Magnetic Fields

B. A. Ioshpa*, V. N. Obridko, and E. A. Rudenchik

Pushkov Institute of Terrestrial Magnetism, Ionosphere, and Radiowave Propagation, Russian Academy of Sciences, Troitsk, Moscow oblast, 142190 Russia

Received August 13, 2007

Abstract—We study the spatial properties of solar magnetic fields using data from the Solar Vector Magnetograph of the Marshall Space Flight Center (MSFC) (Fe I 5250.2 Å) and SOHO/MDI longitudinal magnetic field measurements (Ni 6767.8 Å) (96-min full-disk maps). Our study is focused on two objects: the fractal properties of sunspots and the fractal properties of the spatial magnetic field distribution of active and quiet regions considered as global structures. To study the spatial structure of sunspots, we use a well-known method of determining the fractal dimension based on an analysis of the perimeter–area relation. To analyze the fractal properties of the spatial magnetic field distribution over the solar surface, we use a technique developed by Higuchi. We have revealed the existence of three families of self-similar contours corresponding to the sunspot umbra, penumbra, and adjacent photosphere. The fractal coefficient has maxima near the umbra–penumbra and penumbra–photosphere boundaries. The fractal dependences of the longitudinal and transverse magnetic field distributions are similar, but the fractal numbers themselves for the transverse fields are larger than those for the longitudinal fields approximately by a factor of 1.5. The fractal numbers decrease with increasing mean magnetic field strength, implying that the magnetic field distribution is more regular in active regions.

PACS numbers : 96.60.Q-

DOI: 10.1134/S1063773708030080

Key words: *Sun, solar magnetic fields, fractal analysis.*

FRACTAL PROPERTIES OF SUNSPOTS

Initial Material and the Data Processing Technique

As the initial material, we used data from the Solar Vector Magnetograph of the Marshall Space Flight Center (MSFC) in Huntsville (Alabama, USA) for 2002–2004 (Hagyard et al. 1982; Hagyard and Pevtsov, 1999) available on the Internet. The spatial resolution of these data provided at the MSFC site is 0.7 arcsec. For our analysis, we chose active regions with large sunspots located near the central meridian. For the subsequent processing of the initial data representing the magnetic field strengths at the points of a rectangular grid, we developed a special computer code. This code allowed the following:

(1) to map the photospheric surface brightness distribution in the line used and to superimpose the isolines of the longitudinal magnetic field, isolines of the total magnetic field, isolines of the line-of-sight velocity, and the distribution of transverse magnetic field directions computed by this code on this map (at

our choice) (one of the maps is shown in Fig. 1 as an example);

(2) to calculate the lengths (perimeters) of the magnetic field contours and the areas bounded by these contours;

(3) to select only those isolines that surround the sunspot chosen for our analysis.

Let us briefly describe the last two procedures. The coordinates of the isoline points (i.e., the coordinates of the points of intersection between the isolines and the coordinate grid) were determined by a linear interpolation of the values at the two neighboring grid points between which the isoline passes. The contour length (perimeter) was determined as the sum of the lengths of the segments connecting the isoline points. To estimate the area, we introduced an additional grid consisting of rectangles. The area of the figure bounded by the isoline was calculated as the sum of the areas of the rectangles contained in it. We established whether a rectangle belonged to the figure by looking at the isoline points from the rectangle center. If the sum of the angles at which the points are seen is equal to zero, then the rectangle lies outside the

*E-mail: ioshpa@ttk.ru

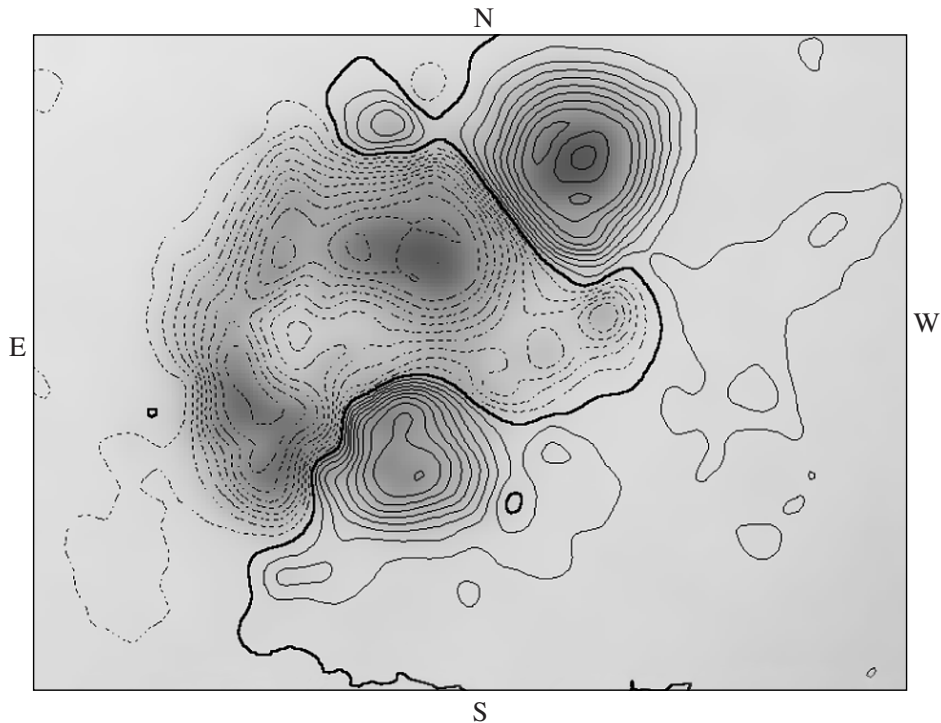


Fig. 1. Map of the longitudinal magnetic field on October 23, 2003 (region 484, N04 S13, MSFC data). The isolines of the longitudinal magnetic field are drawn at 200-G steps. The solid and dashed lines correspond to positive and negative polarities of the longitudinal magnetic field, respectively.

figure; if it is equal to 2π , then the rectangle belongs to the figure and its area is added to the area of the figure. If a particular isoline point falls into the rectangle, then its area enters into to the sum with a weight of 0.5.

We selected the isolines belonging to different sunspots by a special procedure called clustering. Using this code, we divided the isolines into classes corresponding to individual sunspots. The distance between the figures as clustering objects was defined as the distance between their centers of gravity. The object with the largest field strength on the isoline (i.e., the figure closest to the sunspot center) is declared to be a cluster representative. The distance between the object and the cluster is defined as the distance between the object and the cluster representative. If the distance from the object to the cluster is less than its critical value, then the object belongs to the cluster; if the distance is larger than its critical value for all clusters, then the object forms a new cluster. The critical distance is chosen by a visual analysis of the correspondence between clusters and sunspots.

Dependence of the Fractal Dimension on Sunspot Structure Elements

To study the spatial structure of sunspots, we used a well-known method of determining the fractal dimension based on an analysis of the perimeter–area relation for the contours of a magnetic field with various strengths (Feder 1988; Meunier 1999; Nesme-Ribes et al. 1996; Balke et al. 1993). Note that the fractal properties of sunspot magnetic fields were also studied by Zelenyi and Milovanov (1991), Milovanov and Zelenyi (1992), and Mogilevskii (1994, 2001), who considered the sunspots as sets of magnetic clusters.

According to Mandelbrot (1983), the fractal dimension of contours can be determined from the relation between their perimeter L and area S ,

$$L \sim S^{D/2}, \quad 2 \ln L = D \ln S + a, \quad (1)$$

where the parameter D (the so-called Hausdorff dimension) characterizes the contour ruggedness. For example, $D = 1$ for a circle and $D \approx 2$ for a highly rugged contour. If the relation between $2 \ln L$ and $\ln S$ for a particular set of contours is linear, then these contours are considered self-similar.

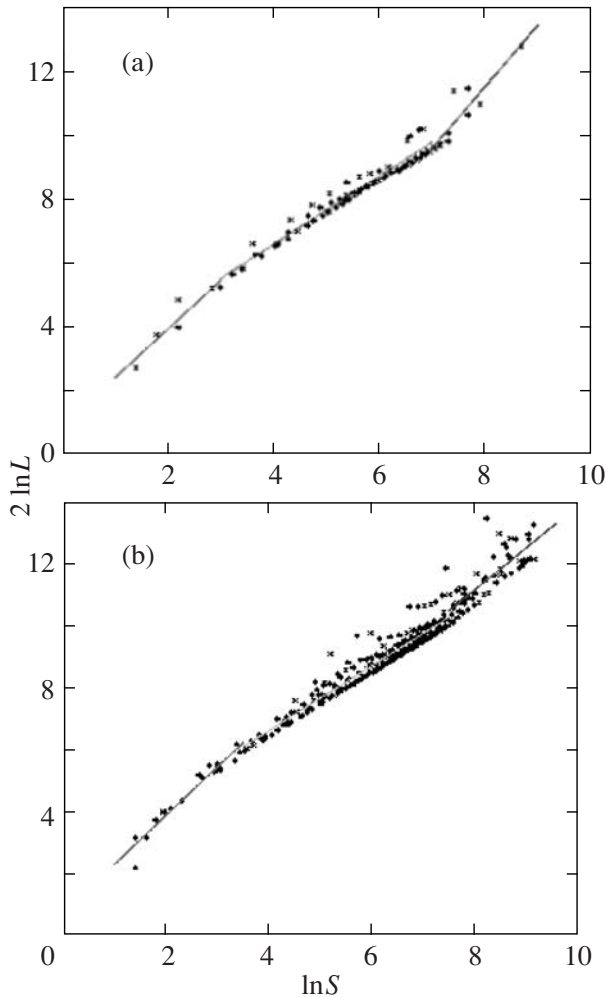


Fig. 2. Dependence of $2 \ln L$ on $\ln S$ for the isolines of the longitudinal (a) and total (b) magnetic fields.

In Fig. 2a, $2 \ln L$ is plotted against $\ln S$ for the isolines of the longitudinal magnetic field for ten large sunspots computed using the above code in the range 2200–400 G at 200-G steps. Generally, these sunspots were largest in each selected region and we restricted our analysis to the region that had the same polarity as this sunspot. We see from Fig. 2a that the $2 \ln L$ – $\ln S$ relation can be fitted by three straight lines: the first, second, and third correspond to $\ln S < 4.5$ ($D = 1.52$), $4.5 < \ln S < 7.5$ ($D = 1.05$), and $\ln S > 7.5$ ($D = 1.93$), respectively (here, L is given in units of the coordinate grid; to obtain L in arcseconds, it must be multiplied by 0.7; accordingly, S must be multiplied by 0.49). This means that the first, second, and third intervals correspond to less than 45 square arcseconds or less than 7 msh, from 45 to 900 square arcseconds or from 7 to 140 msh, and more than 900 square arcseconds or more than

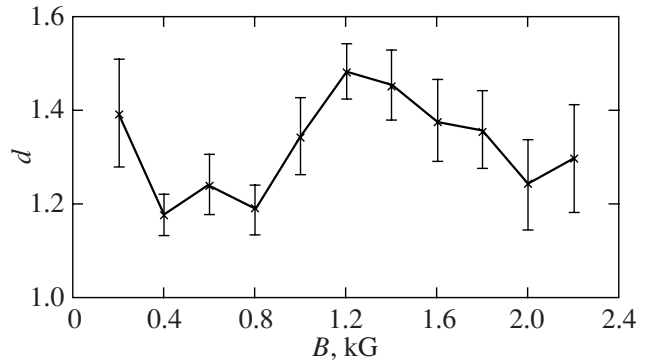


Fig. 3. Fractal index d versus longitudinal magnetic field strength in the range 2200–400 G.

140 msh, respectively. A similar distribution was also obtained for the isolines of the total magnetic field (Fig. 2b). Comparison with the photospheric brightness distribution shows that the first, second, and third intervals roughly correspond to the sunspot umbra or slightly smaller than it, the penumbra, and the outer penumbra and the sunspot-surrounding photosphere, respectively.

This result points to the existence of three families of self-similar magnetic field isolines that roughly correspond to the umbra, penumbra, and the sunspot-surrounding photosphere. As we see, the largest and smallest fractal dimensions correspond to the sunspot-surrounding photospheric region and the sunspot penumbra, respectively. An intermediate fractal index (1.52) corresponds to the sunspot umbra.

Dependence of the Fractal Dimension on the Mean Magnetic Field Strength

We also used a different approach to study the sunspot magnetic structure. It consisted in the following. For all contours of the longitudinal magnetic field in the range 2200–400 G (at 200-G steps), irrespective of which of the sunspots being studied they corresponded, we plotted the $2 \ln L$ – $\ln S$ relations. As our analysis showed, each of these relations was well fitted by a linear function. The slope of this straight line gives the fractal coefficient d that characterizes some averaged quantity corresponding to the contour of a given field strength. We then plotted this coefficient against the longitudinal magnetic field strength (Fig. 3). The figure also shows the standard error. We see that the fractal coefficient has a maximum (close to 1.5) in a region that roughly corresponds to a longitudinal magnetic field strength of 1200 G, which is close to the sunspot umbra–penumbra boundary (Obridko 1985). There is also an

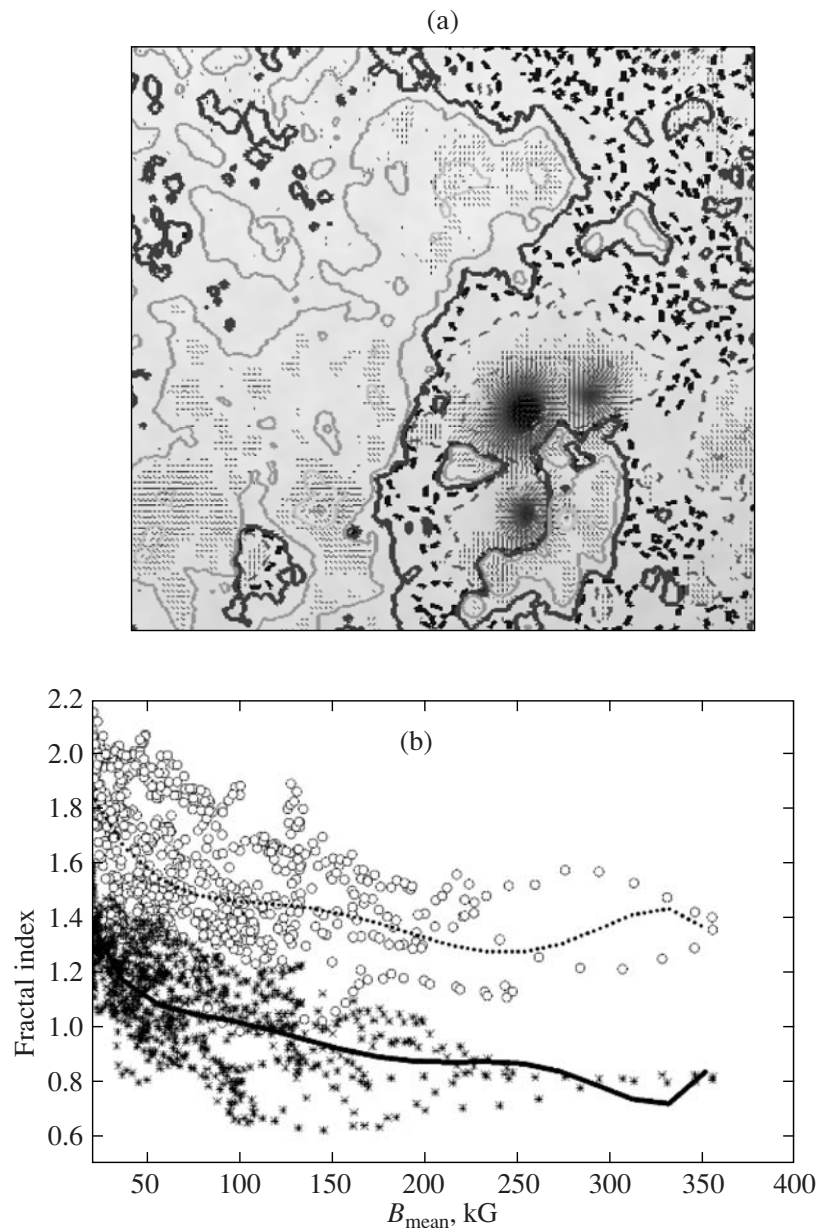


Fig. 4. (a) Magnetic field map obtained with the MSFC Vector Magnetograph on July 7, 2002, for region 19 (S17 W21). (b) Fractal index of the longitudinal (lower curve) and transverse (upper curve) components versus mean absolute value of the longitudinal magnetic field.

increase in the fractal number as the photosphere is approached. Note a discrepancy between the result shown in Figs. 2a and 2b and the result that follows from Fig. 3. As follows from Fig. 3, the maximum of the fractal number in the sunspot umbra obtained by analyzing the slopes of the $2 \ln L - \ln S$ relation shifts toward the umbra–penumbra boundary. This discrepancy (while the results are in general agreement) can most likely be explained by a difference in the averaging methods.

The increase in fractal number at the umbra–penumbra boundary and at the penumbra–photosphere transition (i.e., large ruggedness of the magnetic structure) may be related to the presence of turbulent currents in these regions.

ANALYSIS OF THE FRACTAL PROPERTIES IN AN ACTIVE REGION

The next step in analyzing the fractal structure of the local fields was a study of the fractal properties

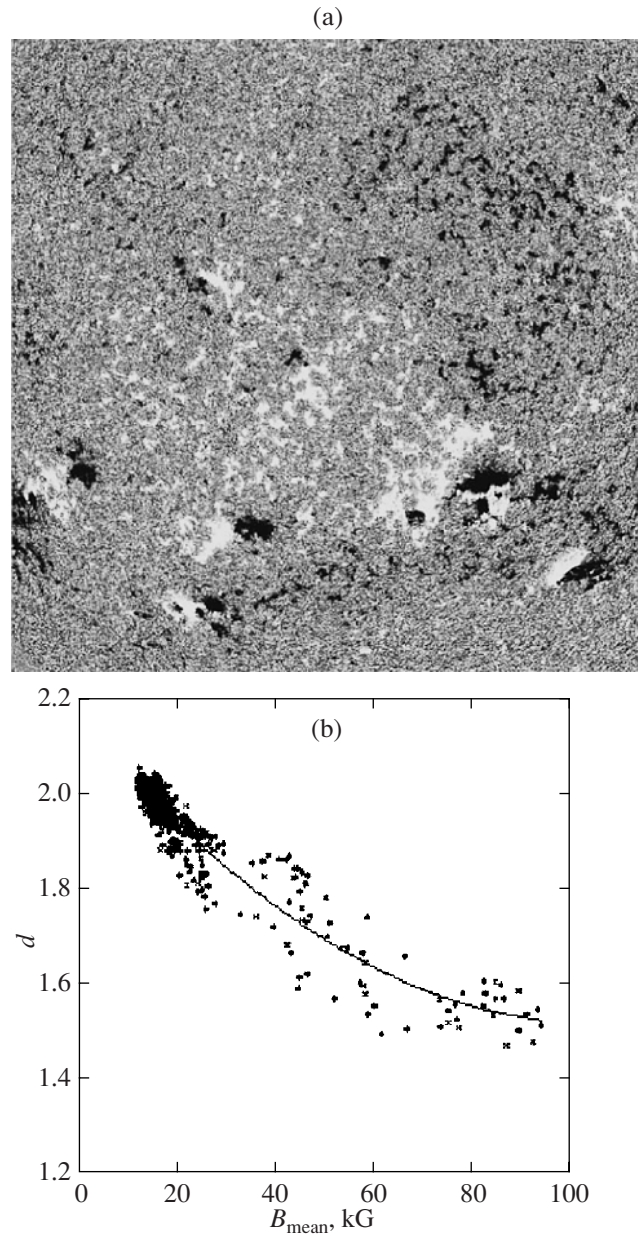


Fig. 5. (a) Longitudinal magnetic field map obtained with the SOHO magnetograph (SOHO/MDI) on July 17, 2002. (b) Fractal index of the longitudinal magnetic field versus mean absolute value of the longitudinal field.

inside an active region. Since here we can no longer orient ourselves to closed contours, we had to change the above technique of calculating the fractal index

and applied the technique used by Higuchi (1988) to analyze long sequences:

$$L_m(k) = \left[\left(\sum_{i=1}^{\left[\frac{N-m}{k} \right]} |X(m+ik) - X(m+(i-1)k)| \right) \frac{N-1}{\left[\frac{N-m}{k} \right] k} \right] / k. \quad (2)$$

Here, $L_m(k)$ is a parameter that characterizes the mean (normalized) distance between the current points, m and k are the initial (moving) point and the interval, respectively, X is the parameter being measured (e.g., the magnetic field, velocity, or brightness), and N is the number of points in the sequence. The logarithm of the mean L_m is related to $\ln k$. As the fractal index, we take the proportionality coefficient D in the relation $\ln\langle L(k)\rangle = -D \ln k + C$.

To compare the fractal numbers of the longitudinal and transverse field distributions, we used data from the MSFC Vector Magnetograph.

The result of this comparison obtained from the magnetic data for one of the days, more specifically, July 7, 2002 (Fig. 4a), is shown in Fig. 4b. The upper and lower curves correspond to the spatial distributions of the transverse and longitudinal field components, respectively. The scan-averaged absolute values of the longitudinal magnetic field are along the horizontal axis. We see that the fractal dependences of the spatial distributions for the transverse and longitudinal fields are similar, but a significant difference is that the fractal indices for the transverse fields are approximately a factor of 1.5 higher than those for the longitudinal fields. This indicates that the spatial distribution of the transverse fields is much more chaotic than that of the longitudinal ones.

FRactal PROPERTIES OF THE SPATIAL DISTRIBUTION OF THE LONGITUDINAL MAGNETIC FIELD OVER THE SOLAR SURFACE

In studying the fractal properties of the magnetic field distribution over the entire solar surface, we also used the technique developed by Higuchi (1988) and Eq. (2).

We analyzed the spatial distribution of the longitudinal magnetic field along various scans of the SOHO/MDI 96-min full-disk magnetic maps (the spatial resolution is 2"; the scans passed through both quiet and active regions (Scherer et al. 1995)). As an example, we present the results obtained by analyzing the magnetic map for July 17, 2002, which contains active complexes that yielded strong solar flares (Fig. 5a). In Fig. 5b, the fractal number of the longitudinal magnetic field distribution for all scans of this map is plotted against the absolute (in sign) value of the field averaged over each scan. We see that for the scans with low mean field strengths, i.e., for the scans passing over relatively quiet solar regions, the fractal index is close to 1.9–2.0, which corresponds to the values that we calculated for white noise. The fractal number decreases with increasing mean field

and falls to 1.5 for the scans that cross active regions with sunspots. This reflects the fact that as the magnetic field strengthens, its spatial distribution becomes less chaotic (more regular). Note that the derived dependence agrees well with the fractal dependence for the longitudinal field shown in Fig. 4b (the initial part of the curve).

CONCLUSIONS

(1) Our fractal analysis of the sunspot magnetic field points to the existence of three families of self-similar magnetic field contours that roughly correspond to the sunspot umbra, penumbra, and adjacent photosphere. The largest and smallest fractal numbers correspond to the region of weak magnetic fields (the photosphere closest to the sunspot) and the penumbra, respectively.

(2) A more detailed analysis shows that the fractal coefficient has a maximum (approximately 1.5) near the umbra–penumbra transition.

(3) The dependences of the fractal numbers for the spatial distributions of the longitudinal and transverse fields over the solar surface are similar in pattern, but the values for the transverse fields are approximately a factor of 1.5 higher than those for the longitudinal ones. Undoubtedly, this result reflects the fact that the transverse fields are distributed over the solar surface much more chaotically than the longitudinal ones.

(4) We established a close correlation of the global fractal indices for the spatial magnetic field distribution over the solar surface with the mean absolute values of the longitudinal magnetic field. The fractal numbers are at a maximum and close to 2.0 (a value characteristic of white noise) for quiet solar regions and decrease to 1.1–1.2 for active regions.

ACKNOWLEDGMENTS

We are grateful to the MSFC and SOHO/MDI staff for the opportunity to use their data stored on the Internet. This work was supported by the Russian Foundation for Basic Research (project nos. 04-02-17007 and 07-02-00333).

REFERENCES

1. A. C. Balke, C. J. Schrijver, C. Zwaan, et al., *Sol. Phys.* **143**, 215 (1993).
2. J. Feder, *Fractals* (Plenum, New York, 1988; Mir, Moscow, 1991).
3. M. J. Hagiard and A. A. Pevtsov, *Sol. Phys.* **189**, 25 (1999).

4. M. J. Hagyard, N. P. Cumings, and J. E. Smith, *Sol. Phys.* **80**, 33 (1982)
5. T. Higuchi, *Physica D* **31**, 277 (1988).
6. B. B. Mandelbrot, *The Fractal Geometry of Nature* (Freeman, New York, 1983).
7. N. Meunier, *Astrophys. J.* **515**, 801 (1999).
8. A. V. Milovanov and L. M. Zelenyi, *Phys. Fluids* **5**, 1406 (1992).
9. E. I. Mogilevskii, *Pis'ma Astron. Zh.* **20**, 607 (1994) [*Astron. Lett.* **20**, 516 (1994)].
10. E. I. Mogilevskii, *Fractals on the Sun* (Fizmatlit, Moscow, 2001) [in Russian].
11. E. Nesme-Ribes, N. Meunier, and D. Collin, *Astron. Astrophys.* **308**, 213 (1996).
12. V. N. Obridko, *Sunspots and Complexes of Solar Activity* (Nauka, Moscow, 1985) [in Russian].
13. P. H. Scherer, R. S. Bogdan, and R. I. Bush, *Sol. Phys.* **162**, 129 (1995).
14. L. M. Zelenyi and A. V. Milovanov, *Pis'ma Astron. Zh.* **17**, 1013 (1991) [*Sov. Astron. Lett.* **17**, (1991)].

Translated by V. Astakhov